# BeFORECAST

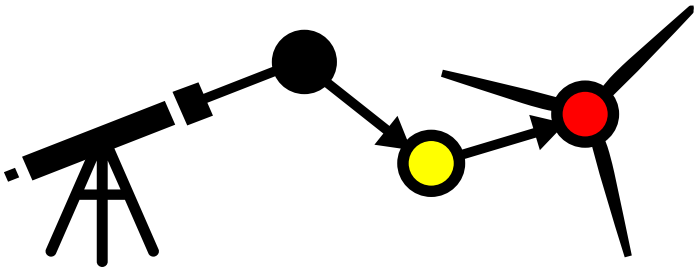

Deliverable: Data assimilation of conventional and novel measurements into mesoscale NWP models

Deliverable No.: D3.1

economie
FOD Economie, K.M.O., Middenstand en Energie

This project has received funding from the Energy Transition Fund of the Belgian Federal Public Service for Economy, SMEs, and Energy (FOD Economie, KMO, Middenstand en Energie)

# DOCUMENT CONTROL SHEET

| DOCUMENT INFORMATION | |
|---|---|
| Document title | Data assimilation of conventional and novel measurements into mesoscale NWP models |
| Author(s), (organization) | Wim Munters (VKI)<br>Geert Smet (RMI)<br>Idir Dehmous (RMI) |
| Deliverable No. | D3.1 |
| Work Package No. | WP3 |
| Lead beneficiary | VKI |
| Dissemination level | Public |
| Date of issue | November 2025 |

## DOCUMENT SUMMARY

This deliverable (D3.1) presents the BeFORECAST project's efforts to improve offshore wind power forecasting through advanced data assimilation techniques in mesoscale numerical weather prediction (NWP) models. The work presented here has been performed in the context of T3.1 and T3.2 of the project. Two complementary approaches are addressed:

- **RMI contribution:** Development and validation of a 3DVar assimilation system within the ALARO model at 1.3 km resolution, integrating conventional observations (SYNOP, AMDAR, TEMP, GNSS-ZTD) and radar-derived radial wind data. Tests during February 2022, including Storm Eunice, show that assimilating radar winds improves short-term wind forecasts, particularly in the Belgian offshore zone. The impact is most pronounced in the first 6–12 hours and is enhanced when combined with wind farm parameterization.

- **VKI contribution:** Application of four-dimensional data assimilation (FDDA) via observational nudging in the WRF model using upstream profiling lidar measurements. Case studies during Storm Eunice and Storm Franklin demonstrate significant reductions in wind speed and direction errors (up to 10.5% RMSE improvement and 2.4× better directional accuracy), leading to more accurate power predictions. Sensitivity analyses highlight best practices for nudging strength and spatial weighting.

Together, these efforts confirm the added value of high-resolution offshore measurements and advanced assimilation strategies for improving short-term wind and power forecasts, supporting grid stability and operational decision-making.

# Table of Contents

# 1 Introduction

The BeFORECAST project aims to enhance the accuracy and reliability of offshore wind power forecasting in the Belgian North Sea. One of the key objectives of the project is to develop and use data assimilation techniques to improve forecasting models of different levels of details and at different timescales. The current deliverable D3.1 provides an overview of the data assimilation efforts in mesoscale numerical weather prediction (NWP) models, with a typical horizontal grid resolution of 1 to 5 km and forecasting time scales of a few hours up to a few days ahead. The work reported here was performed in the context of Tasks T3.1 and T3.2 within Work Package 3.

Data assimilation is a key enabler in improving NWP models. By integrating observational data into model simulations, it allows for a more accurate representation of the atmospheric state, especially in regions with sparse measurements like offshore wind farms. In the context of NWP, data assimilation typically refers to the ingestion of observations from satellites, radars, weather stations, and other sources in a mathematical model to improve the global accuracy of the initial condition of the weather model, hence facilitating a more truthful representation of the atmospheric state at model initialization. In the current report, we also explore a different type of data assimilation, i.e. observational nudging, which adds local forcing terms to the dynamical equations to force the wind field closer to reference observations.

The remainder of this deliverable is structured as follows. Section 2 discusses the state-of-the-art assimilation techniques developed and used in operational models at RMI in the conventional data assimilation setting. Section 3 elaborates on an alternative approach used by VKI to assimilate local profiling lidar data into the Weather, Research and Forecasting model using observational nudging (so called four-dimensional data assimilation, FDDA). The goal is to demonstrate the added value of high-resolution offshore measurements for improving wind and power forecasts. Further, Section 4 provides a high-level summary of the activities and Section 5 provides an overview of the dissemination activities associated to this deliverable.

# 2 Data assimilation in RMI weather models

At RMI, data assimilation developments have followed a clear trajectory, moving from early experiments with AROME to the current focus on ALARO (Termonia et al., 2018) at convection-permitting resolution of 1.3 km. The first milestone was the installation of a full surface data assimilation cycle in AROME (June 2020). The aim was to combine a surface analysis provided by CANARI (Code d'ARPEGE Necessaire A ses Rejets et son Initialisation) for more accurate surface and soil (temperature and moisture) fields and a 3DVar analysis.

The background error covariance matrix (B) was evaluated using both the NMC method (Parrish and Derber, 1992) and ensemble-based statistics from the EDA (Brousseau et al., 2011). Building on this, the assimilation framework was relatively basic since it used only conventional observations such as SYNOP, AMDAR and TEMP. Among these, GNSS data from the E-GVAP network were assimilated using the status bias approach. Despite these advances, difficulties persisted in the representation of wind, particularly near the surface, therefore two cycling strategies such as digital filter initialization (DFI) and incremental analysis update (IAU) were tested without fully resolving the issue. Nonetheless, these efforts culminated in the installation of an AROME 3DVar system in a pre-operational configuration. Some investigations on the AROME SURFEX revealed a suboptimal tuning of the model dynamic and physics near the boundary layer.

Recently, the efforts have concentrated on ALARO at 1.3 km resolution which has a more refined tuning of dynamical and physical processes near the surface. A pure 3DVar cycle has been established with the ISBA scheme for surface processes and assimilates conventional observations (SYNOP, AMDAR, TEMP) and remote sensing such as ZTD (Zenith Total Delay) from GNSS stations. The ALARO 1.3 km 3DVar currently serves as the principal platform for testing new assimilation strategies at RMI.

In section 2.1 we shortly describe the 3DVar system, focusing on conventional data. The further assimilation of radial wind from weather radars, particularly relevant for offshore wind energy, is explained in section 2.2. This is then applied to ALARO at 1.3 km, with and without wind farm parameterization (Van den Bleeken et al., 2025), which is further described in BeFORECAST deliverable *D4.2 Intercomparison of mesoscale models including wind-farm parameterization implementations.* Validation results of these experimental model runs in the Belgian offshore zone (BOZ) are summarized in section 2.3. We summarize here only those results from internal RMI reports (Dehmous, 2025a; Dehmous, 2025b) that are relevant for the BeFORECAST project.

## 2.1 The 3DVar data assimilation system

The purpose of a data assimilation scheme is to optimally combine the available observations with a short-term model forecast in order to estimate the most probable state **x** of the atmosphere at a given time. In a 3DVar system, a cost function (Lorenc 1986):

$$J(\mathbf{x}) = \frac{1}{2}(\mathbf{x} - \mathbf{x}^b)^{\mathrm{T}}\mathbf{B}^{-1}(\mathbf{x} - \mathbf{x}^b) + \frac{1}{2}(\mathbf{y} - \mathcal{H}(\mathbf{x}))^{\mathrm{T}}\mathbf{R}^{-1}(\mathbf{y} - \mathcal{H}(\mathbf{x}))$$

is minimized at a single time (in 3D space). The cost function is defined as the distance between **x** (the true atmospheric state) and the background $\mathbf{x^b}$, weighted by the inverse of the background error covariance **B**, plus the distance to the observations **y**, weighted by the inverse of the observation error covariance **R**.
Solving the variational problem consists in finding the minimum of the function J as :

$$\nabla J(X) = 0$$

**x:** Control variables - the atmospheric state we want to estimate
$\mathbf{x^b}$ **:** Background or first guess - short range previous forecast
**B:** Model or background errors covariances
**R:** Observations errors covariances
**H:** the observation operator - interpolate the model variables to observation space
**y:** The observations vector.

The NMC method (Parrish and Derber, 1992) provides a practical way to estimate the background error covariance matrix **B** using existing model forecasts. It assumes that the differences between two forecasts valid at the same time but with different lead times can approximate the statistics of forecast errors.

The implemented 3DVar at RMI is still relatively simple, as it assimilates only a limited set of upper-air observations: AMDAR, TEMP, GNSS-ZTD, and MODE-S data. However, the assimilation operates with a 3-

hour rapid update cycling to maintain frequent and consistent adjustment of the model state to observations.
The SYNOP, AMDAR and TEMP are assimilated directly, however the GNSS needed a pre-treatment to evaluate the static of each station and are assimilated using a static bias correction of the parameter ZTD (Zenith Total Delay). Figure 1 shows the ALARO Belgium 3DVar observation coverage and figure 2 shows the daily number of received observations.

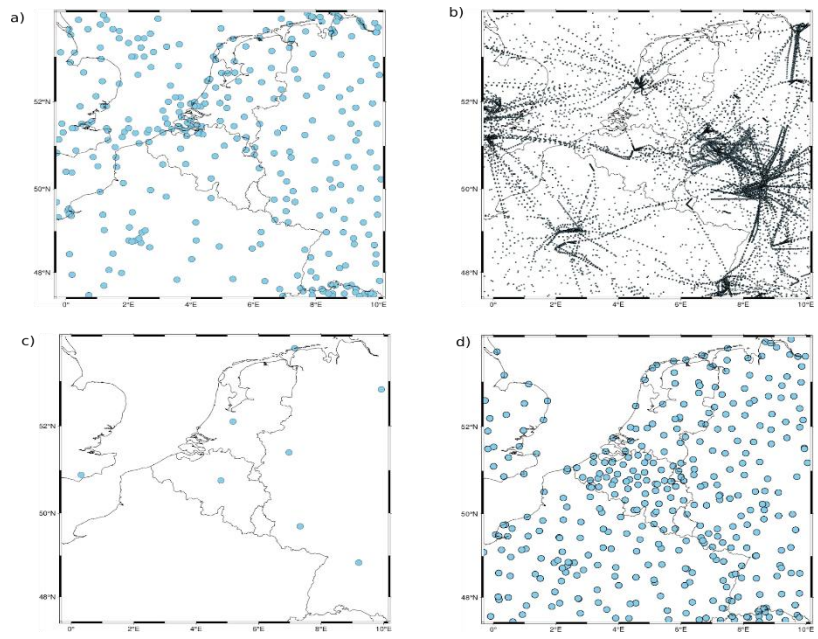


*Figure 1: ALARO Belgium 3DVar observation coverage.*

The 3DVar system consists of a 3-hour intermittent data assimilation and production cycle. Every 3 hours the observations are combined with the 3 hours forecast produced by the previous cycle (First guess). The observations are converted to the ODB (Observation DataBase) format. The ODB is compared to the first guess (the screening step) in order to check the data quality and is flagged according to their level of uncertainty. The screening represents the last quality control check before the introduction of the observations into the minimisation and the production of the analysis, as shown in figure 3.

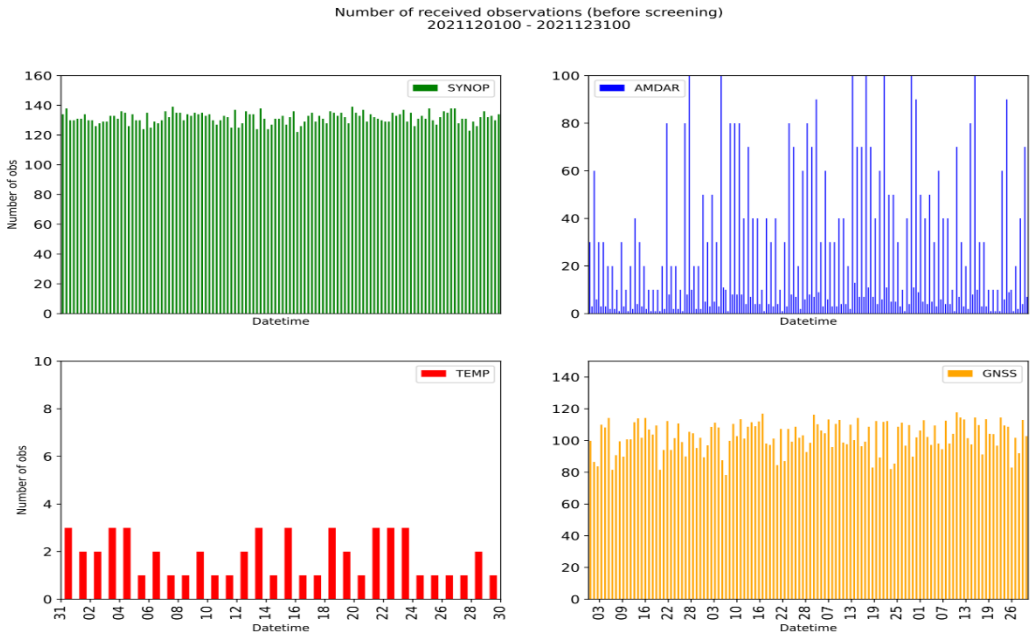


*Figure 2: Daily number of received observations (raw observations before assimilation).*

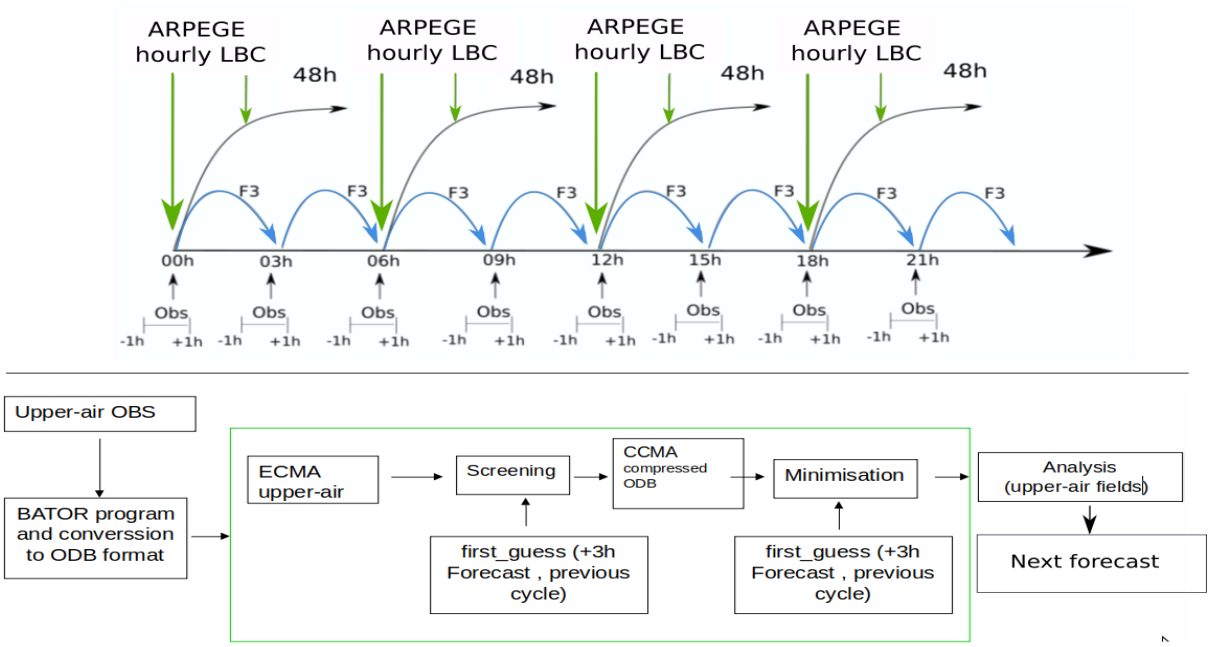


*Figure 3: ALARO 3DVar cycling strategy.*

The observations and model error handling is crucial in a 3DVar system. They are represented by their covariances/correlations matrices noted as **R** and **B** respectively. Due to the large size of the system in NWP models, **B** cannot be explicitly written and stored. The **B** matrix is modeled by different operators. For more details please refer to Parrish et al. (1997) for global model and Berre (2000) for LAM under

some assumptions (homogeneity, isotropy, stationarity etc ). The relative weights between **B** and **R** determine how much trust is given to the background versus the observations. To diagnose and tune the system, the Desroziers diagnostic method (Desroziers and Ivanov, 2001; Desroziers, 2005) was used to assess the consistency between background, observation, and analysis errors.

## 2.2 Assimilation of radar radial wind

The study of radar-derived data has become increasingly important for enhancing short-term weather forecasts, especially within high-resolution numerical weather prediction (NWP) systems such as ALADIN. One of the radar products which can be assimilated within high resolution NWP models is the Doppler radial wind (VRAD). The measurements provide direct wind components along the radar beam, thereby offering valuable information on the three-dimensional atmospheric flow. Nevertheless, their assimilation into operational models remains challenging because of significant variability in data quality, spatial coverage, and consistency between different radar sites and networks.

The available RMI radar data is shown in figure 4 and table 1, and further described in BeFORECAST deliverable D1.1 *Overview of BeFORECAST field and virtual measurement campaigns*.

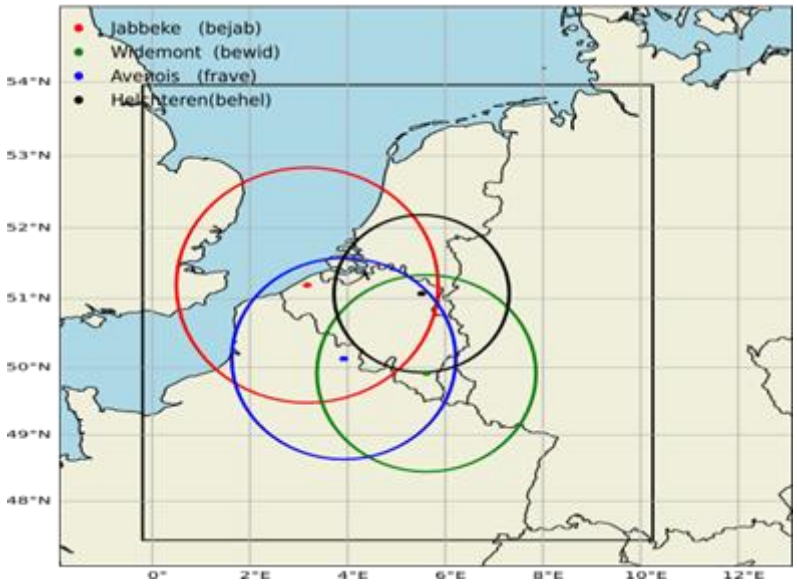


*Figure 4: The Belgian radar coverage and ALARO 1.3Km domain.*

| radar | Location | Latitude (deg) | Longitud (deg) | Altitude (m) | Band | Dual pol | Max range (Km) | Doppler |
|---|---|---|---|---|---|---|---|---|
| **bejab** | Jabbeke | 51.1919 | 3.0641 | 50 | C | Yes | 240 | Yes |
| **bewid** | Wideumont | 49.9135 | 5.5044 | 585 | C | No | 240 | Yes |
| **behel** | Helchteren | 51.0702 | 5.4054 | 144 | C | Yes | 200 | No |
| **bezav** | Zaventem | 50.9654 | 4.4579 | 73 | C | No | 240 | No |
| **frave** | Avesnois | 50.1283 | 3.8118 | 191 | C | Yes | 256 | Yes |

*Table1: Available RMI radar data.*

The radar obtains the radial velocity of the target by measuring the impulse phase difference between transmitted and received signals (Doppler-Fizeau effect). However, velocity ambiguity can result in wrong data assimilation and wrong field retrieval. The Nyquist velocity represents the maximum unambiguous velocity that the radar can measure without aliasing. Aliasing occurs when higher velocities appear to be lower due to the limitations of the radar sampling rate. This happens because the radar samples the Doppler shift at discrete intervals determined by the pulse repetition frequency. The maximum radial wind that can be measured without aliasing is given by

$$V_{max} = \frac{4\ \mathrm{PRF}}{\lambda},$$

where PRF is the Pulse-Repetitive Frequency and $\lambda$ the radar wavelength. Table 2 summarizes the Nyquist velocity for those radars where quality flags for radial wind are available. Note the low Nyquist velocity for radar 'behel', which was therefore excluded in further data assimilation experiments.

| Radar | Low PRF (Hz) | Middle PRF (Hz) | High PRF (Hz ) | Nyquist velocity (m/s) |
|---|---|---|---|---|
| **bejab (Jabbeke)** | 800 | – | 1000 | 53.50 |
| **bewid (Wideumont)** | 960 | – | 1200 | 63.84 |
| **behel (Helchteren)** | 0 | – | 550 | 7.35 |
| **frave (Avenois)** | 440 | 489 | 550 | 58.58 |

*Table 2: RMI radar data for which the quality flags for radial wind are available.*

In the first attempts to include the radial velocities from radars the results were not satisfactory. A few issues were identified as non-optimal in the data assimilation, all of them allowing bad quality data to enter the data assimilation. According to the diagnostics, these reasons can be summarized as follows

- Gross observations errors
- Multi-modal errors distribution often showing heavy tails
- Non gaussian distribution of the errors which is not consistent with the assumptions made in the 3DVar minimization

Therefore, complementary approaches were introduced. A First Guess Check is applied to identify and reject observations with excessively large departures from the background. In addition, the histogram transform method (Anderson and Jarvinen, 1999) was tested to “Gaussianize” the distribution of VRAD innovations. By mapping the histogram onto a normal distribution using an empirical function, this technique allows the departures to better satisfy the Gaussian error assumption underlying 3DVar, and provides a more consistent treatment of radar observations in the assimilation system.

The tuning of observation errors is a further crucial step in the assimilation of radar radial winds. Following the method of Desroziers (Desroziers et al., 2005), the ratios of innovation and residual variances were

analysed to adjust the observation-error statistic. In addition, the very high spatial density of radar observations requires the application of a spatial thinning procedure. Without thinning, the assimilation system would treat strongly correlated data points as independent, thereby over-constraining the analysis. Following the approach of (Liu and Rabier 2003), the thinning distance was chosen such that the correlation falls below 0.2.

## 2.3 Validation results in the Belgian offshore zone

The above 3DVar assimilation of conventional data, and radar radial wind was tested with the ALARO 1.3 km model in February 2022, chosen in part because of the occurrence of storm Eunice during this test period. Experiments with and without the wind farm parameterization (WFP) in ALARO (Van den Bleeken et al, 2025) enabled were carried out, as summarized in table 3. For the validation, we restrict here to results for an anonymous wind farm in the BOZ, although positive impact over land is also seen (but not relevant for BeFORECAST).

| Exp name | Initialisation | WFP enabled | Assimilated observations (conventional) | Radial wind VRAD assimilated |
|---|---|---|---|---|
| **AO13D15** | First ARPEGE LBC | **NO** | None | None |
| **AO13F15** | 3DVAR | **NO** | SYNOP, AMDAR, TEMP, GPSSOL | **NO** |
| **AO13RW1** | 3DVAR | **NO** | SYNOP, AMDAR, TEMP, GPSSOL | **YES** |
| **AO13WD1** | First ARPEGE LBC | **YES** | None | None |
| **AO13WF1** | 3DVAR | **YES** | SYNOP, AMDAR, TEMP, GPSSOL | **NO** |
| **AO13RWF** | 3DVAR | **YES** | SYNOP, AMDAR, TEMP, GPSSOL | **YES** |

*Table 3: ALARO 1.3km experiments to test 3DVAR and VRAD assimilation.*

The experiments without WFP are compared in figures 5 and 6, showing BIAS and MAE respectively. Both figures clearly show 3DVAR improving upon the downscaling experiment (AO13WD1), and the additional benefit of assimilating VRAD. While the positive impact of conventional data seems to last (only) about 6 hours, the assimilation of VRAD has a much longer impact, lasting almost 24 hours, but then seemingly having a somewhat negative impact.

A different picture is seen in the experiments with WFP enabled, as shown in figures 7 and 8. Now the impact of VRAD becomes neutral after about 12 hours, and in the early part of the forecast, the positive impact of 3DVAR and VRAD becomes less clear and at times somewhat negative. However, despite the unclear impact on MAE in figure 8, note that both 3DVAR and VRAD still lead to an improved bias in the first 6 hours, as seen in figure 7, and will generally lead to a better initial state. Assimilating VRAD (with WFP) should therefore also be recommended when creating a local high resolution, which can be useful for climate analysis, wind energy resource assessment and development of AI weather models. Specific tuning of the 3DVAR and VRAD assimilation with the WFP enabled might also still lead to further improvements, to be investigated in the future.

Note also the very positive effect of switching on the wind farm parameterization in ALARO, leading to much lower bias and MAE in figures 7 and 8, when comparing with the scores in figures 5 and 6. This will be further discussed in BeFORECAST deliverable *D4.2 Intercomparison of mesoscale models including wind-farm parameterization implementations.*

Finally, the impact of the 3DVAR and VRAD assimilation during storm Eunice is shown in figures 9 and 10, for the experiments without and with the WFP respectively. They show similar results, with the 3DVAR and VRAD experiments lying somewhat closer to the observations in the first 3 hours of the forecast, and very little difference between the experiments after 6 to 9 hours. Overall, the VRAD experiments seem slightly better than the 3DVAR (and downscaling) experiments. In general, the peak of the storm and overall time evolution was well predicted by all the model experiments. Some overestimation of the wind speed is also seen between lead times 6h and 14h, which is somewhat reduced in the WFP experiments. In conclusion, the 3DVAR and VRAD assimilation seem to have mostly positive effects.

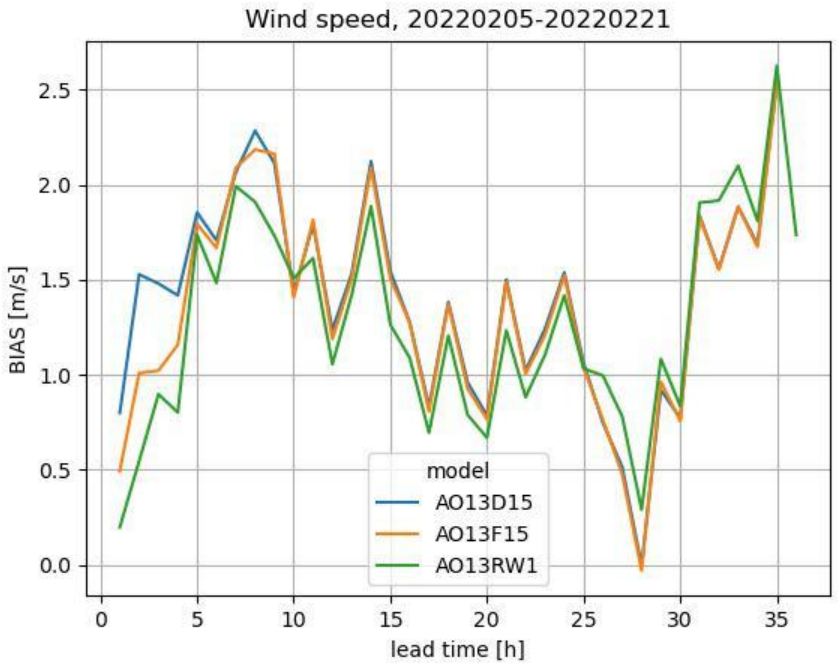


*Figure 5: BIAS of 100m wind speed forecasts for ALARO 1.3km (downscaling, 3DVAR and VRAD) experiments without WFP, averaged over the period 5 February–21 February 2022, evaluated against lidar observations from an anonymous wind farm in the BOZ.*

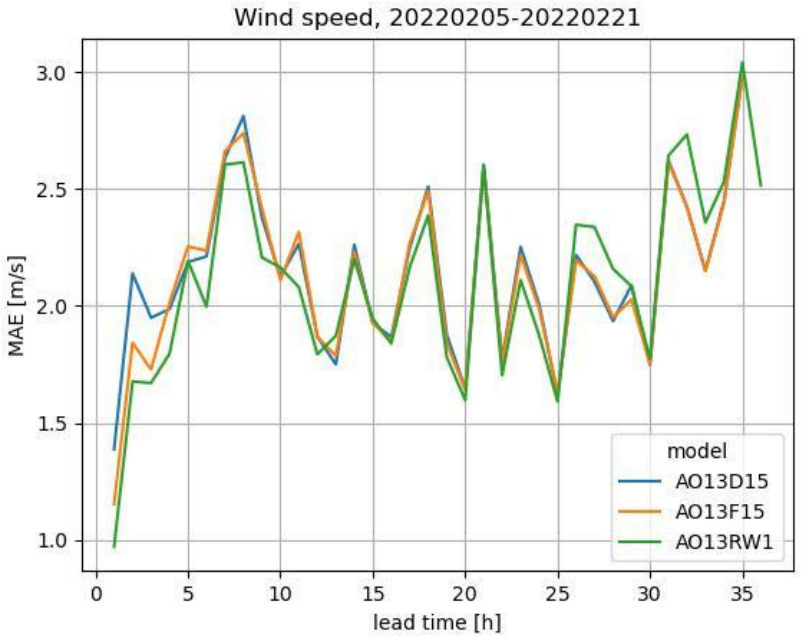


*Figure 6: MAE of 100m wind speed forecasts for ALARO 1.3km (downscaling, 3DVAR and VRAD) experiments without WFP, averaged over the period 5 February–21 February 2022, evaluated against lidar observations from an anonymous wind farm in the BOZ.*

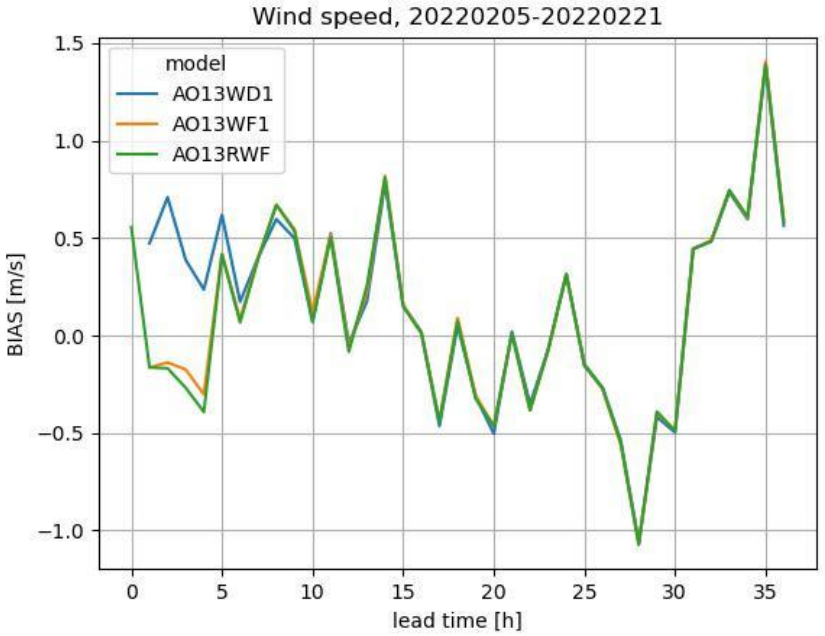


*Figure 7: BIAS of 100m wind speed forecasts for ALARO 1.3km (downscaling, 3DVAR and VRAD) experiments with WFP, averaged over the period 5 February–21 February 2022, evaluated against lidar observations from an anonymous wind farm in the BOZ.*

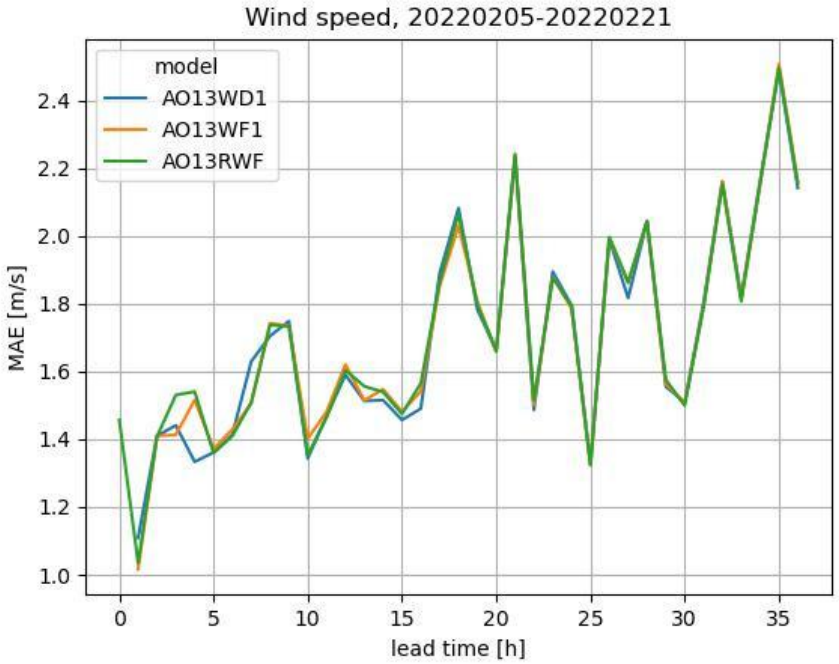


*Figure 8: MAE of 100m wind speed forecasts for ALARO 1.3km (downscaling, 3DVAR and VRAD) experiments with WFP, averaged over the period 5 February–21 February 2022, evaluated against lidar observations from an anonymous wind farm in the BOZ.*

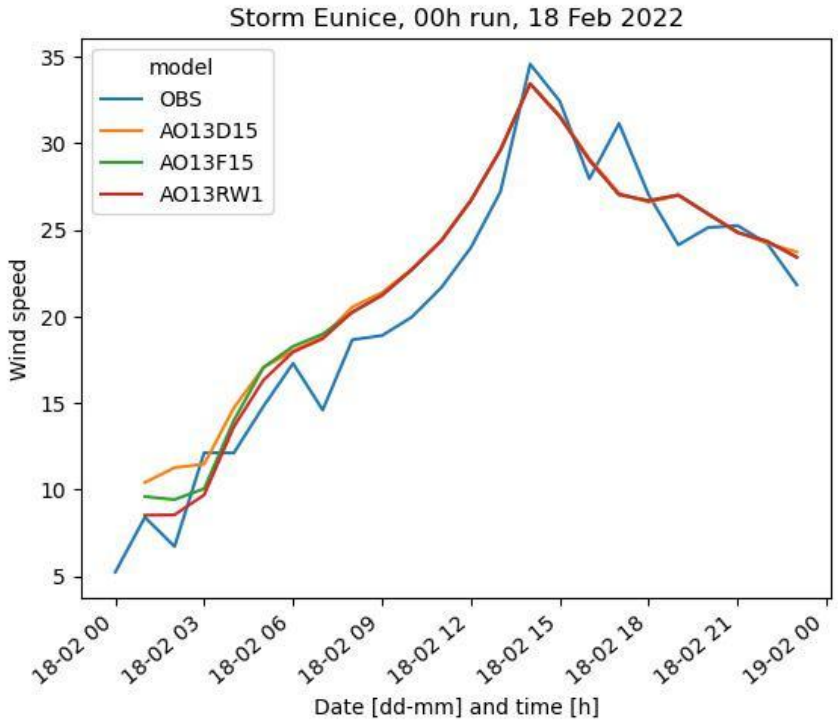


*Figure 9: Time series of 100m wind speed forecasts for ALARO 1.3km (downscaling, 3DVAR and VRAD) experiments without WFP, for 18 February 2022, during storm Eunice. Observations from lidar at an anonymous wind farm in the BOZ, in blue.*

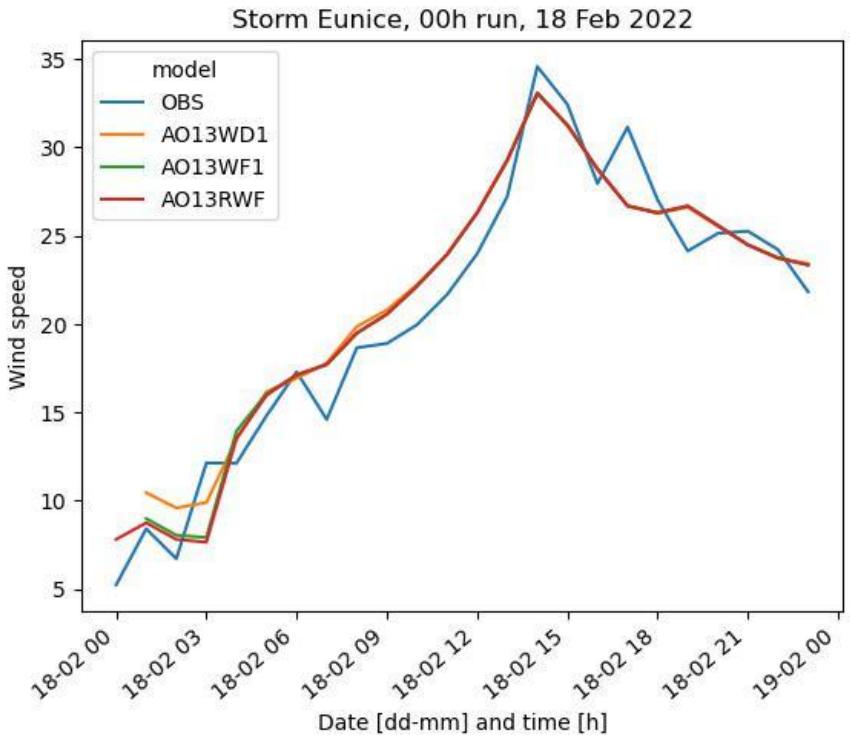


*Figure 10: Time series of 100m wind speed forecasts for ALARO 1.3km (downscaling, 3DVAR and VRAD) experiments with WFP, for 18 February 2022, during storm Eunice. Observations from lidar at an anonymous wind farm in the BOZ, in blue.*

# 3 Data assimilation of profiling lidar data in WRF weather model (VKI)

The current section summarizes the FFDA / nudging work performed by the VKI in a case study to enhance wind and power forecasting for offshore wind farms based on a case study of extreme events in February 2022. The full technical detail is available in the peer-reviewed and open-access journal paper:

- Ivanova, T., Porchetta, S., Buckingham, S., Glabeke, G., van Beeck, J., and Munters, W.: Improving wind and power predictions via four-dimensional data assimilation in the WRF model: case study of storms in February 2022 at Belgian offshore wind farms, Wind Energ. Sci., 10, 245–268, https://doi.org/10.5194/wes-10-245-2025 , 2025

## 3.1 Introduction and methodology

Recent advancements in offshore measurement technologies, particularly the deployment of profiling lidars, have opened new possibilities for improving weather forecasts in wind farm regions. VKI has explored the assimilation of these lidar observations into the WRF model using a FDDA technique, also known as observational nudging.

Although several studies have investigated the use of FDDA for offshore wind energy with wind turbine anemometers (Cheng et al., 2017) or met masts (Mylonas et al., 2018), the currently described work of Ivanova et al. (2025) is the first to assess the nudging of wind speed and wind direction measurements from a profiling lidar located strategically upstream of an offshore wind farm.

Figure 11 illustrates the spatial extent of the setup of the study. The ZX 300M lidar is operated by the VKI and installed on the Westhinder platform (cf. BeFORECAST Deliverable D1.1 for further information). Measurement data at a height of 104.5 m above mean sea level is used for nudging the model at a height

of 104.5 m, similar to the typical hub height of an offshore wind turbine in the Belgian-Dutch wind farm cluster. As observed in the wind rose, the lidar is located upstream of the wind farm, considering the southwesterly prevailing wind direction.

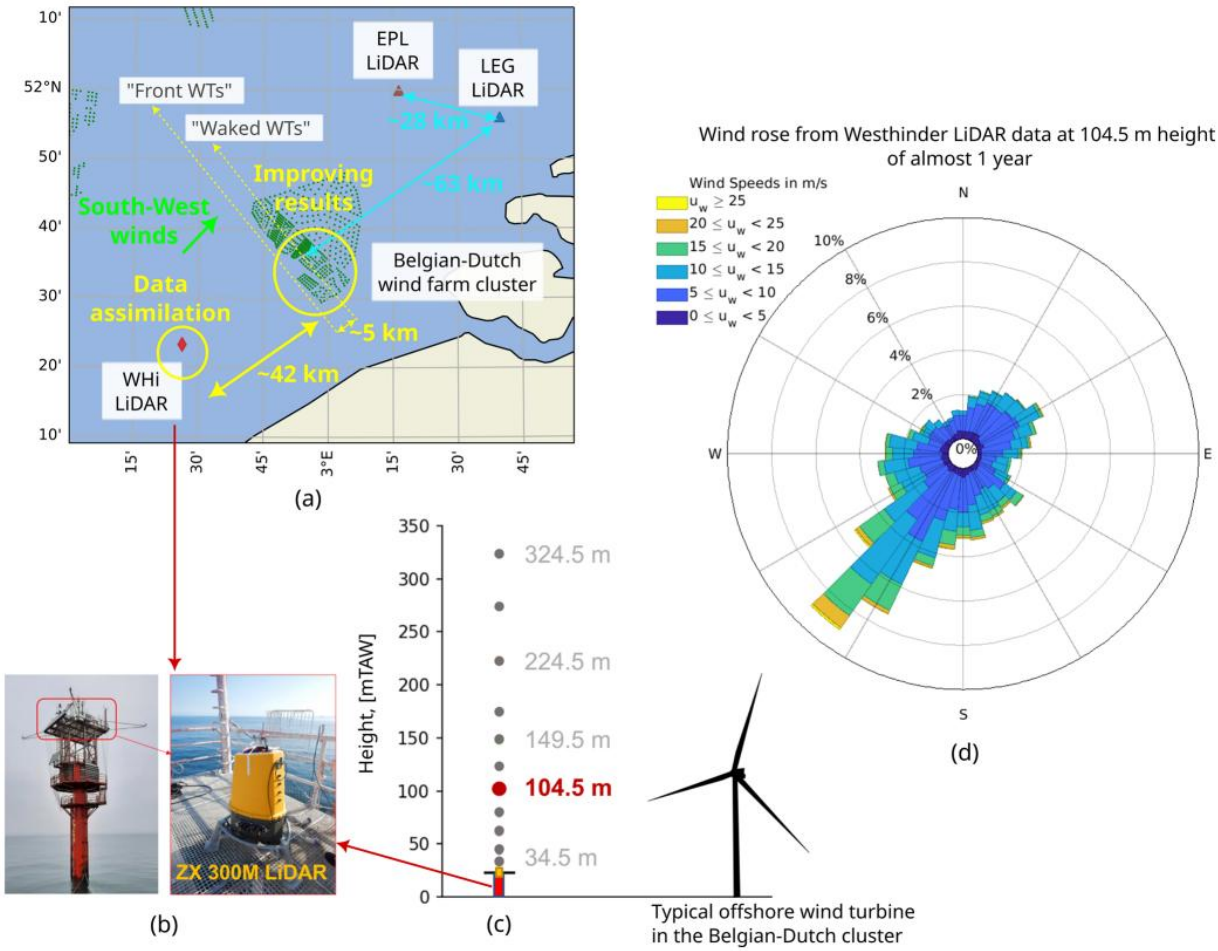


*Figure 11: Overview of case study setup. (a) Location of lidar for nudging (Whi) and model evaluation (EPL and LEG). (b) VKI WHi lidar installed on the Westhinder platform. (c) Measurement heights of the lidar, with nudging data shown in red, compared to the typical height of a wind turbine in the Belgian-Dutch cluster. (d) Wind rose obtained from the lidar campaign at the Westhinder location.*

Simulations are performed with the open-source public domain WRF model (Skamarock et al. 2019). A typical physics configuration is used in combination with the Fitch parameterization (Fitch et al. 2014). Further details can be found in the paper and in Deliverable D4.2. The model readily implements FDDA / nudging capabilities through the possibility of adding a forcing term to the dynamical equations as

$$\frac{\partial q\mu}{\partial t} = F_q + \mu\, G_q\, W_q(q_o - q),$$

where $q$ is the model variable to be forced (in our case the components of horizontal wind speed), $F_q$ are the physical model tendencies (e.g. due to advection, turbulence, convection, etc.), $\mu$ is the dry hydrostatic pressure, $G_q$ is a scalar nudging strength, $W_q$ is a spatiotemporal weighting function localizing the force

on the simulation domain, and $q_o$ is the observation value of the model variable under consideration. The formula shows that this nudging acts as a proportional controller locally forcing the model variable $q$ to its observation $q_o$. A sensitivity study to the nudging parameters $G_q$ and $W_q$ is performed in the paper to identify best practices.

Several model runs are performed, both with and without nudging. Model performance is measured by computing standard metrics Mean Absolute Error (MAE), Root-Mean-Square-Error (RMSE), and bias with respect to downstream observations from both wind turbine anemometers and lidar platforms LEG and EPL (see Figure 11).

## 3.2 Case Study: February 2022 Storms

The approach was tested during a series of storm events in February 2022, impacting several critical infrastructures in Western Europe, including the Belgian–Dutch wind farm cluster in the Southern Bight of the North Sea. Specifically, the focus is on the occurrence of Storm Eunice and Storm Franklin. Figure 12 shows lidar wind speed measurements at 104.5 m above mean sea level during the time period of interest. Storm Eunice features a peak 10-min averaged wind speed of 37.14 m/s, which is the highest wind speed measured during the VKI measurement campaigns, whereas Storm Franklin has a peak velocity of 30.46 m/s, followed by a sharp decrease in wind speed and a strong shift in the wind direction.

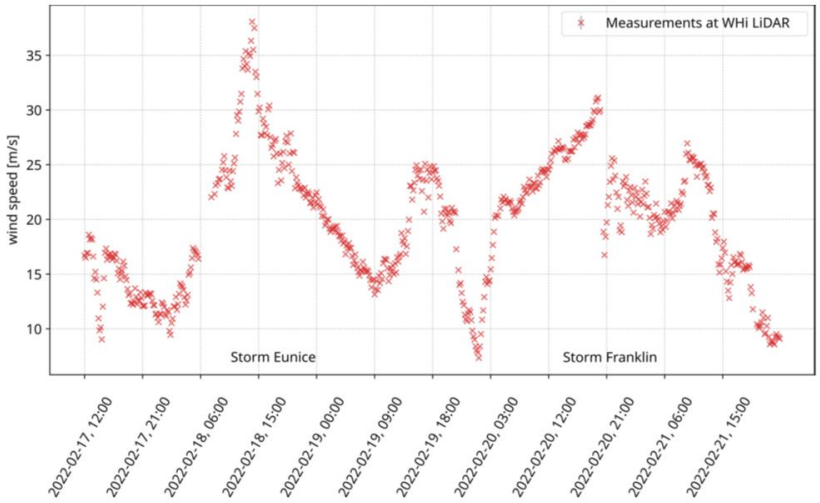


*Figure 12: Lidar wind speed measurements at 104.5m above mean sea level during Storm Eunice and Storm Franklin.*

## 3.3 Key results and Findings

An example of the effect of the nudging is illustrated in Figure 13. The baseline simulation (left) panel was found to underpredict wind speed at the Westhinder lidar location, whereas the middle panel shows that through nudging (FDDA), the wind speed is increased both at the lidar location and downstream (northeast) of the lidar. Note that the forcing is non-physical (and in this case with strong forcing parameters) and can introduce non-local artefacts in the model as well (right panel). However, it is shown that the procedure can be used to drive the model to higher wind speeds, both locally and downstream.

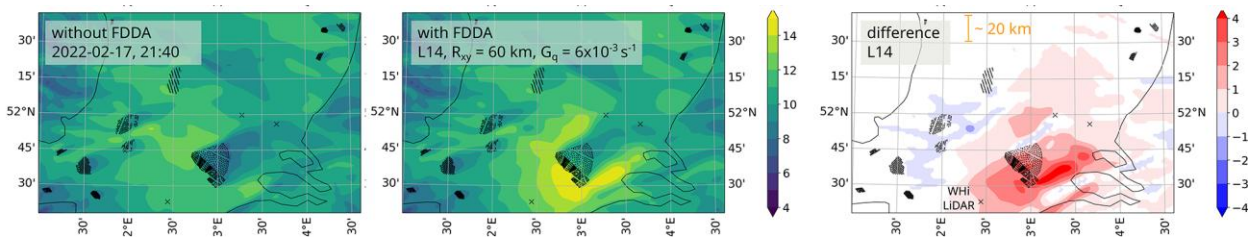


*Figure 13: Snapshots of wind speed fields on 17 February 21:40 UTC. Left: baseline simulation without FDDA. Middle: simulation with FDDA. Right: Difference between left and middle panel. Colors are in units of m/s and the x depicts the WHi lidar location. Black dots represent the parameterized wind turbines in the simulations.*

Full technical details and results can be found in the paper and are omitted here for brevity. As an example, we show the RMSE and bias metrics for wind speed in Figure 14. Every row in this figure represents a single simulation with different nudging parameters $G_q$ and $W_q$, whereas every column represents its error metric compared to wind turbine measurements as well as downstream lidars EPL and LEG. The figure illustrates that, depending on the chosen parameters, both RMSE and bias can be reduced significantly at the downstream observations of the nudging location Westhinder.

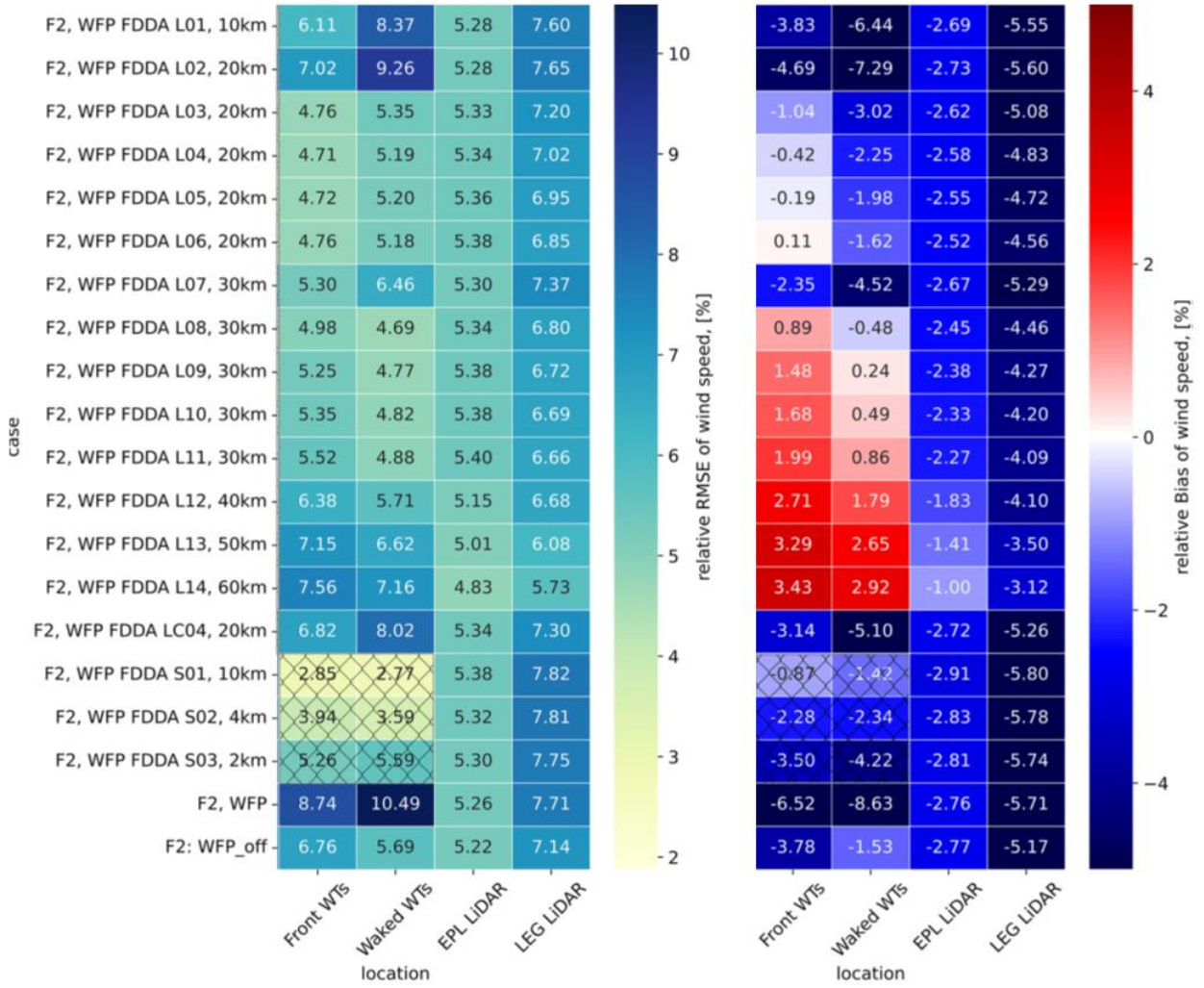


*Figure 14: (Left) Relative RMSE of wind speed of reference simulation (F2 WFP) and FDDA cases. (Right) Same, for wind speed bias.*

The overall insights and implications of the paper can be summarized as follows:

1. Assimilation of lidar wind observations significantly reduced wind errors: reductions in wind speed RMSE have been observed from 10.5% (F2, WFP) to 5.2% (case L04, L05, L06). For wind direction, errors were shown to be improved by up to a factor 2.4.
2. These improved wind speed and wind direction forecasts led to more accurate power production estimates, especially for turbines affected by wake effects.
3. Sensitivity studies on nudging parameters helped identify suitable configurations for offshore nudging of upstream local measurements in weather models.

These results were used in further case studies to highlight the potential of lidar-based assimilation to enhance hour-ahead forecasts, which are critical for operational decision-making in offshore wind farms. The study also underscores the importance of upstream measurements and the spatial configuration of sensors in maximizing forecast improvements.

# 4 Conclusion

The work presented in this deliverable demonstrates that data assimilation is a key enabler for improving offshore wind forecasting in mesoscale NWP models. RMI's implementation of 3DVar with conventional and radar observations in ALARO enhances short-term wind predictions, particularly during high-impact events such as Storm Eunice. While the benefits of radar assimilation are clear in the early forecast hours, further tuning is needed to optimize performance when wind farm parameterization is active.

VKI's FDDA approach using upstream lidar data in WRF shows strong potential for reducing wind and power forecast errors, especially under extreme conditions. The results underline the importance of spatial sensor placement and parameter sensitivity in achieving robust improvements. Both studies confirm that integrating novel offshore measurements into NWP systems can significantly improve forecast accuracy and reliability.

Future work could focus on combining these techniques, refining assimilation strategies for operational use, and exploring hybrid approaches that leverage both conventional and novel data sources. These advancements will contribute to safer, more efficient offshore wind farm operations and better integration of renewable energy into the power grid.

# 5 Dissemination

- Ivanova, T., Porchetta, S., Buckingham, S., Glabeke, G., van Beeck, J., and Munters, W.: Improving wind and power predictions via four-dimensional data assimilation in the WRF model: case study of storms in February 2022 at Belgian offshore wind farms, Wind Energ. Sci., 10, 245–268, https://doi.org/10.5194/wes-10-245-2025 , 2025

# 6 References


Anderson, E. and Järvinen, H. (1999), Variational quality control. Q.J.R. Meteorol. Soc., 125: 697-722. https://doi.org/10.1002/qj.49712555416

Berre, Loïk (2000). "Estimation of Synoptic and Mesoscale Forecast Error Covariances in a Limited-Area Model". *Mon. Wea. Rev.*, **128**, 644–667, https://doi.org/10.1175/1520-0493(2000)128<0644:EOSAMF>2.0.CO;2.

Brousseau, P., Berre, L., Bouttier, F. and Desroziers, G. (2011), Background-error covariances for a convective-scale data-assimilation system: AROME–France 3D-Var. Q.J.R. Meteorol. Soc., 137: 409-422. https://doi.org/10.1002/qj.750

Cheng, W.Y., Liu, Y., Bourgeois, A.J., Wu, Y. and Haupt, S.E., 2017. Short-term wind forecast of a data assimilation/weather forecasting system with wind turbine anemometer measurement assimilation. Renewable Energy, 107, pp.340-351.

Derber, J. and F. Bouttier (1999), A reformulation of the background error covariance in the ECMWF global data assimilation system. *Tellus A: Dynamic Meteorology and Oceanography*, *51*(2), 195–221. https://doi.org/10.3402/tellusa.v51i2.12316

Dehmous, I. (2025a), The ALARO Belgium 3DVAR Part I : The Tuning. Internal report of the Royal Meteorological Institute of Belgium.

Dehmous, I. (2025b), ALARO Belgium 3DVAR Part II: Assimilation of the radar radial wind. Internal report of the Royal Meteorological Institute of Belgium.

Desroziers, G. and Ivanov, S. (2001), Diagnosis and adaptive tuning of observation-error parameters in a variational assimilation. Q.J.R. Meteorol. Soc., 127: 1433-1452. https://doi.org/10.1002/qj.49712757417

Desroziers, G., Berre, L., Chapnik, B. and Poli, P. (2005), Diagnosis of observation, background and analysis-error statistics in observation space. Q.J.R. Meteorol. Soc., 131: 3385-3396. https://doi.org/10.1256/qj.05.108

Ivanova, T., Porchetta, S., Buckingham, S., Glabeke, G., van Beeck, J., and Munters, W.: Improving wind and power predictions via four-dimensional data assimilation in the WRF model: case study of storms in February 2022 at Belgian offshore wind farms, Wind Energ. Sci., 10, 245–268, https://doi.org/10.5194/wes-10-245-2025, 2025

Liu, Z.-.-Q. and Rabier, F. (2003), The potential of high-density observations for numerical weather prediction: A study with simulated observations. Q.J.R. Meteorol. Soc., 129: 3013-3035. https://doi.org/10.1256/qj.02.170

Lorenc, A. C. (1986), Analysis methods for numerical weather prediction. Q.J.R. Meteorol. Soc., 112: 1177-1194. https://doi.org/10.1002/qj.49711247414

Mylonas, M.P., Barbouchi, S., Herrmann, H. and Nastos, P.T., 2018. Sensitivity analysis of observational nudging methodology to reduce error in wind resource assessment (WRA) in the North Sea. *Renewable Energy*, *120*, pp.446-456.

Parrish, D. and J. Derber (1992), The National Meteorological Center's Spectral Statistical-Interpolation Analysis System. Mon. Wea. Rev., 120, 1747–1763, https://doi.org/10.1175/1520-0493(1992)120<1747:TNMCSS>2.0.CO;2.

Parrish, David F. et al. (1997), The NCEP Global Analysis System: Recent Improvements and FuturePlans (Special Issue Data Assimilation in Meteorology and Oceanography: Theory and Practice). Journal of the Meteorological Society of Japan. Ser. II 75.1B, pp. 359–365.https://doi.org/10.2151/jmsj1965.75.1B_359

Skamarock, W. C., Klemp, J. B., Dudhia, J., Gill, D. O., Liu, Z., Berner, J., Wang, W., Powers, J. G., Duda, M. G., Barker, D. M., and Huang, X.-Y.: A Description of the Advanced Research WRF Model Version 4.3, NSF [code], https://doi.org/10.5065/1DFH-6P97, 2019

Termonia, P., Fischer, C., Bazile, E., Bouyssel, F., Brožková, R., Bénard, P., Bochenek, B., Degrauwe, D., Derková, M., El Khatib, R., Hamdi, R., Mašek, J., Pottier, P., Pristov, N., Seity, Y., Smolíková, P., Španiel, O., Tudor, M., Wang, Y., Wittmann, C., and Joly, A.: The ALADIN System and its canonical model configurations AROME CY41T1 and ALARO CY40T1, Geosci. Model Dev., 11, 257–281, https://doi.org/10.5194/gmd-11-257-2018, 2018.

Van den Bleeken, D., Smet, G., Van den Bergh, J., Dehmous, I., Degrauwe, D., Van Ginderachter, M., and Deckmyn, A.: Improving wind power forecasts in the Belgian North Sea with a wind farm parameterization and a neural network, Adv. Sci. Res., 22, 59–67, https://doi.org/10.5194/asr-22-59-2025, 2025.